8. R. S. Scott *et al*., *Nature* **411**, 207 (2001).
9. V. A. Fadok *et al*., *Nature* **405**, 85 (2000).
10. S. Arur *et al*., *Dev. Cell* **4**, 587 (2003).
11. J. C. Clark *et al*., *Proc. Natl. Acad. Sci. U.S.A.* **92**, 7794 (1995).
12. M. J. Kresch, C. Christian, F. Wu, N. Hussain, *Pediatr. Res.* **43**, 426 (1998).
13. L. M. Scavo, R. Ertsey, C. J. Chapin, L. Allen, J. A. Kitterman, *Am. J. Respir. Cell Mol. Biol.* **18**, 21 (1998).
14. M. E. De Paepe *et al*., *J. Pediatr. Surg.* **34**, 863 (1999).
15. M. O. Li, M. R. Sarkisian, W. Z. Mehal, P. Rakic, R. A. Flavell, data not shown.
16. C. Y. Kuan, K. A. Roth, R. A. Flavell, P. Rakic, *Trends Neurosci.* **23**, 291 (2000).
17. R. W. Oppenheim, *Annu. Rev. Neurosci.* **14**, 453 (1991).
18. K. Kuida *et al*., *Nature* **384**, 368 (1996).
19. K. Kuida *et al*., *Cell* **94**, 325 (1998).
20. R. Hakem *et al*., *Cell* **94**, 339 (1998).
21. F. Cecconi, G. Alvarez-Bolado, B. I. Meyer, K. A. Roth, P. Gruss, *Cell* **94**, 727 (1998).
22. H. Yoshida *et al*., *Cell* **94**, 739 (1998).
23. V. A. Fadok, G. Chimini, *Semin. Immunol.* **13**, 365 (2001).
24. J. Savill, I. Dransfield, C. Gregory, C. Haslett, *Nature Rev. Immunol.* **2**, 965 (2002).
25. A. A. Manfredi, M. Iannacone, F. D'Auria, P. Rovere-Querini, *Apoptosis* **7**, 153 (2002).
26. J. R. Leonard, B. J. Klocke, C. D'Sa, R. A. Flavell, K. A. Roth, *J. Neuropathol. Exp. Neurol.* **61**, 673 (2002).
27. P. W. Reddien, S. Cameron, H. R. Horvitz, *Nature* **412**, 198 (2001).
28. D. J. Hoeppner, M. O. Hengartner, R. Schnabel, *Nature* **412**, 202 (2001).
29. F. S. Cole, A. Hamvas, L. M. Nogee, *Pediatr. Res.* **50**, 157 (2001).

30. We thank M. Pypaert and C. Marks at the Yale EM facility for technical assistance; L. Evangelisti, C. Hughes, and J. Stein for their help in creating the PSR-deficient mice; F. Manzo for preparing the manuscript; and C. Zeiss and C. Iwema for technical assistance. Supported by the Howard Hughes Medical Institute (R.A.F.), National Institute of Neurological Disorders and Stroke (P.R.), and American Heart Association (P.R.).

Supporting Online Material

www.sciencemag.org/cgi/content/full/302/5650/1560/DC1
Materials and Methods
Figs. S1 to S5
Table S1
References and Notes

4 June 2003; accepted 8 October 2003

Cell Corpse Engulfment Mediated by *C. elegans* Phosphatidylserine Receptor Through CED-5 and CED-12

Xiaochen Wang[1]* Yi-Chun Wu,[2]*† Valerie A. Fadok,[3] Ming-Chia Lee,[2] Keiko Gengyo-Ando,[4] Li-Chun Cheng,[2] Duncan Ledwich,[1] Pei-Ken Hsu,[2] Jia-Yun Chen,[2] Bin-Kuan Chou,[2] Peter Henson,[3] Shohei Mitani,[4] Ding Xue[1]†

During apoptosis, phosphatidylserine, which is normally restricted to the inner leaflet of the plasma membrane, is exposed on the surface of apoptotic cells and has been suggested to act as an "eat-me" signal to trigger phagocytosis. It is unclear how phagocytes recognize phosphatidylserine. Recently, a putative phosphatidylserine receptor (PSR) was identified and proposed to mediate recognition of phosphatidylserine and phagocytosis. We report that *psr-1*, the *Caenorhabditis elegans* homolog of PSR, is important for cell corpse engulfment. In vitro PSR-1 binds preferentially phosphatidylserine or cells with exposed phosphatidylserine. In *C. elegans*, PSR-1 acts in the same cell corpse engulfment pathway mediated by intracellular signaling molecules CED-2 (homologous to the human CrkII protein), CED-5 (DOCK180), CED-10 (Rac GTPase), and CED-12 (ELMO), possibly through direct interaction with CED-5 and CED-12. Our findings suggest that PSR-1 is likely an upstream receptor for the signaling pathway containing CED-2, CED-5, CED-10, and CED-12 proteins and plays an important role in recognizing phosphatidylserine during phagocytosis.

Although the important role of phosphatidylserine (PS) in presenting apoptotic cells for phagocytosis is well established (*1*–*10*), the mechanism by which it is recognized by phagocytes to trigger the phagocytosis event remains elusive. To investigate the potential involvement of PSR in recognizing PS and in removing apoptotic cells, we characterized the *C. elegans* PSR homolog, *psr-1*, which is defined by an open reading frame F29B9.4 and encodes a 400–amino acid protein with 56% sequence identity and 72% sequence similarity to the human PSR protein (fig. S1) (*11*). In an enzyme-linked immunosorbent assay (ELISA), recombinant PSR-1, produced and purified from *Escherichia coli*, preferentially bound PS over phosphatidylinositol (PI), phosphatidylethanolamine (PE), or phosphatidylcholine (PC) and displayed a binding preference to phospholipids similar to that of human PSR (Fig. 1A). Thus, PSR-1 appears to be a PS-specific binding protein. Human Jurkat T lymphocytes transiently transfected with worm PSR-1 bound to apoptotic Jurkat T cells or symmetric red blood cell

[1]Department of Molecular, Cellular, and Developmental Biology, University of Colorado, Boulder, CO 80309, USA. [2]Institute of Molecular and Cellular Biology, National Taiwan University, Taipei, Taiwan 10617. [3]Program in Cell Biology, Department of Pediatrics, National Jewish Medical and Research Center, Denver, CO 80206, USA. [4]Department of Physiology, Tokyo Women's Medical University, School of Medicine, Tokyo, 162-8666, Japan.

*These authors contributed equally to this work.
†To whom correspondence should be addressed. E-mail: ding.xue@colorado.edu, yichun@ntu.edu.tw

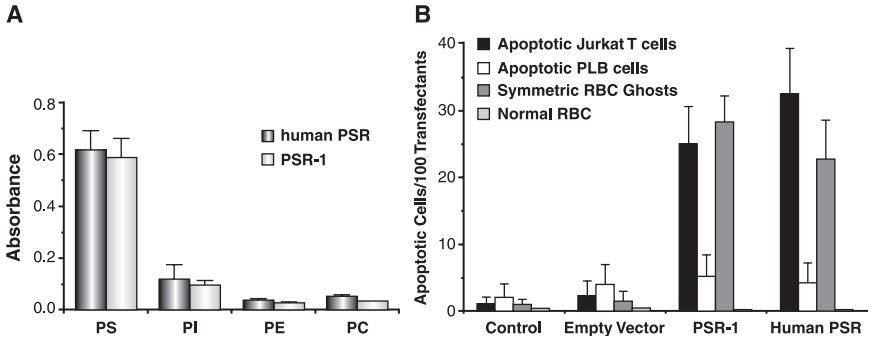

Fig. 1. Phosphatidylserine binding by *C. elegans* PSR-1. (**A**) Preferential binding of PS by recombinant PSR-1 and human PSR proteins in an ELISA assay. PSR-1 and human PSR proteins were expressed in *E. coli* and purified as described (*13*). Microtiter plates were coated with lipids as described (*27*). PSR-1 or human PSR (100 μg) was added to quadruplicate wells for each lipid and incubated overnight at 4°C. Bound protein was detected with monoclonal antibody 217G8E9; the binding of this antibody to PSR-1 was supported by equivalent absorbance results using an antibody to His_6 to detect the N-terminal polyhistidine tag on PSR-1 (*28*). Results represent the mean ± SEM of four separate experiments, with quadruplicate data points from each experiment. PI, phosphatidylinositol; PE, phosphatidylethanolamine; PC, phosphatidylcholine. (**B**) Human Jurkat T lymphocytes transiently transfected with PSR-1 bind to PS-expressing apoptotic cells and red blood cell ghosts. Jurkat cells were transfected with either the PSR-1– or the human PSR–expressing vector (*13*), then examined after 48 hours for their ability to bind to apoptotic Jurkat T cells (PS+), apoptotic PLB 985 cells (PS−) (*12*), symmetric red blood cell (RBC) ghosts (PS+), and normal red blood cells (PS−). Binding was quantified by light microscopy. Binding experiments were performed on cells obtained from three separate transfections. Within each experiment, binding was assessed in triplicate. Data are expressed as the mean ± SEM. Transfection efficiency was 27.5 ± 5.6%.

ghosts, both of which have surface-exposed PS. Such transfected T cells did not bind to apoptotic PLB 985 cells or normal red blood cells (Fig. 1B), which lack surface-exposed PS (*12*). These observations indicate that PSR-1 can recognize and bind to PS or cells with surface-exposed PS in *C. elegans*.

We investigated the potential involvement of *psr-1* in removing cell corpses in *C. elegans* by examining a mutant strain containing a 968–base pair (bp) deletion (*tm469*) in the *psr-1* locus that results in the removal of most of the PSR-1 protein, except its first 14 amino acids (*13*). In a time-course analysis of cell corpses during development (*14*), in almost all embryonic stages, more cell corpses were observed in *psr-1(tm469)* embryos than in wild-type embryos (Fig. 2A). This increase in cell corpses did not appear to be a result of ectopic cell death because *psr-1(tm469)* animals contained the same number of nuclei in their anterior pharynx as did wild-type animals (*15*). In some specific cell lineages, cells that are programmed to die actually survived in *psr-1(tm469)* animals (*16*). The increase of embryonic cell corpses in the *psr-1(tm469)* mutant could be caused by a defect in cell corpse engulfment. We therefore used four-dimensional microscopy analysis to measure the duration of persistence of embryonic cell corpses in *psr-1(tm469)* animals. On average, cell corpses of *psr-1(tm469)* embryos persisted for 55% longer than those of wild-type animals (Fig. 2B). These results indicate that the cell corpse engulfment process is compromised in the *psr-1(tm469)* mutant.

As a cell surface receptor, PSR is proposed to act in engulfing cells to recognize exposed PS on apoptotic cells and mediate

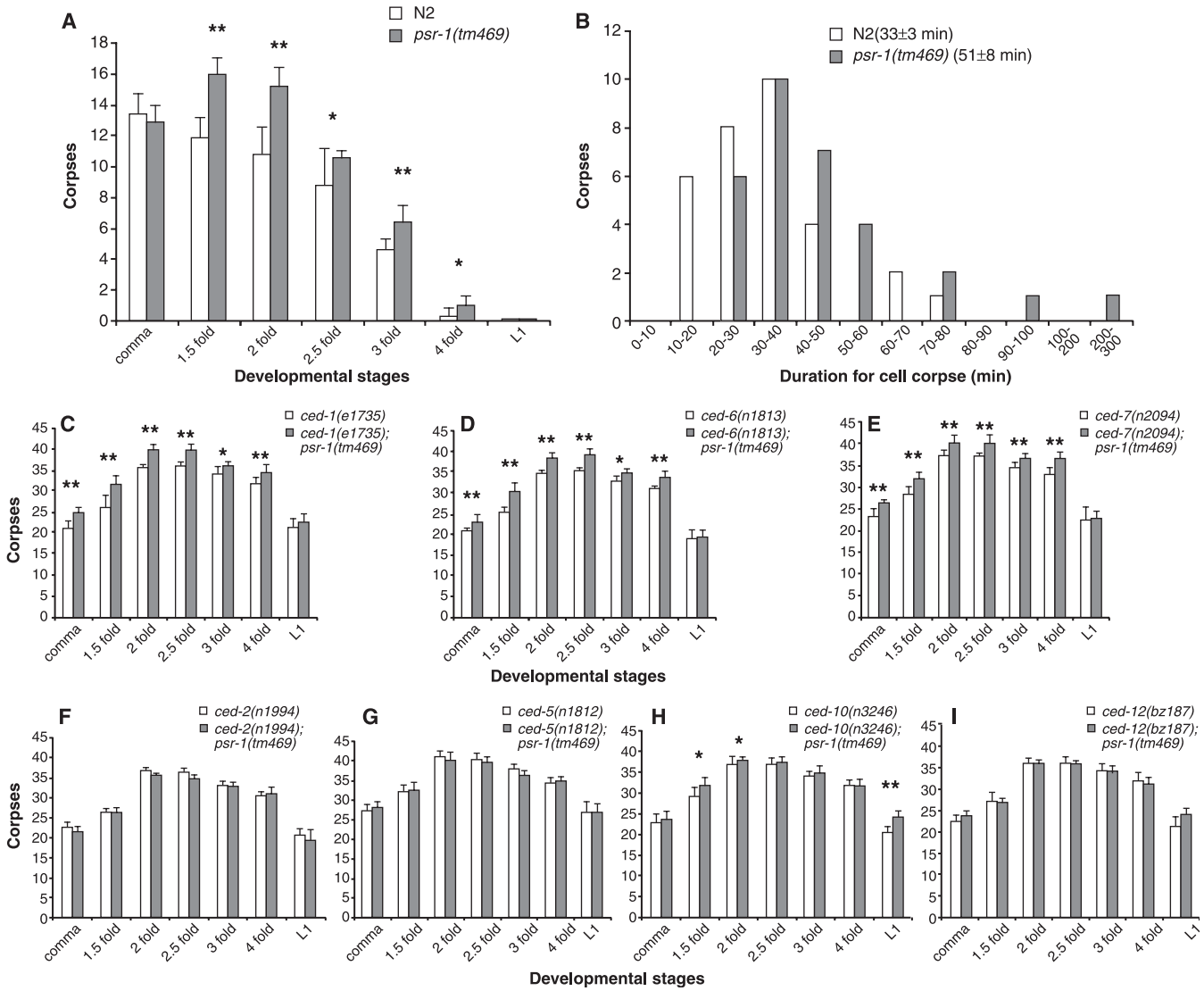

Fig. 2. Importance of *psr-1* for cell corpse engulfment in *C. elegans*. (**A**) Time-course analysis of cell corpses during development. (**B**) Four-dimensional microscopy analysis of durations of persistence of cell corpses. The persistence of 31 cell corpses each from N2 embryos (n = 4, open bars) and *psr-1(tm469)* embryos (n = 3, filled bars) was monitored. The numbers in parentheses indicate the average persistence for cell corpses (±SEM) from each genotype. The y axis indicates the number of cell corpses within a specific duration range (shown on the x axis). The durations of four cell divisions in the MS cell lineage from the MS cell to the MS.aaaa cell (*29*) were also followed to ensure that the embryos assayed had similar rates of development. The average duration of four cell divisions for N2 embryos is 85 ± 3 min and 80 ± 4 min for *psr-1(tm469)* embryos. (**C** to **I**) The *psr-1(tm469)* mutation enhances the engulfment defect of *ced-1*, *ced-6*, and *ced-7* mutants. In (A) and (C) to (I), cell corpses from the indicated animals were scored at comma, 1.5-fold, 2-fold, 2.5-fold, 3-fold, and 4-fold embryonic stages and in L1 larval stage. The y axis represents the mean number of cell corpses scored at the head region of embryos or larvae (15 animals at each developmental stage). Error bars represent the standard deviation. In each panel, data derived from two different genetic backgrounds at multiple developmental stages were compared by two-way analysis of variance. Post hoc comparisons were done by Fisher's PLSD (protected least squares difference). *$P < 0.05$, **$P < 0.0001$. All other points had P values > 0.05.

their phagocytosis (*10*, *11*). We thus tested whether PSR-1 acts in engulfing cells to promote cell-corpse engulfment. Expression of PSR-1 in the *psr-1(tm469)* mutant under the control of the promoter of the *ced-1* gene ($P_{ced\text{-}1}$*psr-1*) [which is expressed in cell types acting as engulfing cells but not in dying cells (*17*)] fully rescued the corpse engulfment defect of the *psr-1* mutant (Table 1). Therefore, *psr-1* likely functions in engulfing cells to promote phagocytosis of cell corpses. Overexpression of human PSR in the *psr-1* mutant using the *C. elegans* heat-shock promoters (P_{hsp}hPSR) also partially rescued the *psr-1* engulfment defect (Table 1), suggesting that the function of PSR in mediating removal of apoptotic cell corpses is likely conserved.

In *C. elegans*, two partially redundant pathways mediate cell corpse removal, with *ced-1*, *ced-6*, and *ced-7* genes functioning in one pathway and *ced-2*, *ced-5*, *ced-10*, and *ced-12* genes acting in the other (*18*–*21*). To examine the functioning pathway of *psr-1*, we constructed and analyzed double mutants between the *psr-1(tm469)* mutation and the strong loss-of-function alleles of the above seven *ced* genes. The *psr-1(tm469)* mutation specifically enhanced the corpse engulfment defect of the *ced-1*, *ced-6*, or *ced-7* mutants but not that of the *ced-2*, *ced-5*, *ced-10*, or *ced-12* mutants, indicating that *psr-1* likely acts in the same cell corpse engulfment pathway as *ced-2*, *ced-5*, *ced-10*, and *ced-12* (Fig. 2, C to I).

The *ced-2*, *ced-5*, *ced-10*, and *ced-12* genes function in engulfing cells and encode homologs of Crk II, DOCK180, Rac guanosine triphosphatase (GTPase), and ELMO, respectively, all of which are important intracellular signaling molecules (*19*–*23*). CED-2, CED-5, and CED-12 appear to form a ternary signaling complex in response to upstream engulfment signals and activate the small GTPase CED-10 to initiate the rearrangement of cytoskeleton necessary for the cell corpse engulfment process (*19*–*21*, *24*). Overexpression of *ced-2*, *ced-5*, *ced-10*, *ced-12*, or *psr-1* gene itself in *psr-1(tm469)* mutants with the *C. elegans* heat-shock promoters rescued the *psr-1* engulfment defect (Table 1). In contrast, overexpression of *ced-1*, *ced-6*, or *ced-7*, which act in a different engulfment pathway, did not rescue the engulfment defect in *psr-1(tm469)* mutants (Table 1). These results suggest that *psr-1* likely acts upstream of *ced-2*, *ced-5*, *ced-10*, and *ced-12* to control the engulfment of cell corpses.

To investigate how *psr-1* might act to transduce the engulfment signal, we examined whether PSR-1 physically interacted with CED-2, CED-5, CED-10, or CED-12 in a yeast two-hybrid assay. The intracellular domain of PSR-1 (PSR-1-IN) interacted specifically with CED-5 and CED-12 but not with CED-2 or CED-10 (Fig. 3A). These interactions were also observed in pull-down assays with glutathione *S*-transferase (GST) fusion proteins. Because CED-5 is a large protein and was not readily expressed in vitro, we dissected it into two regions for in vitro expression: CED-5A (amino acids 1 to 1414) and CED-5B (amino acids 1415 to 1781). A portion of ^{35}S-methionine–labeled CED-5A or CED-5B (about 5 to 10% of

Table 1. Rescue of cell corpse engulfment defect of the *psr-1* mutant by overexpression of CED-2, CED-5, CED-10, or CED-12. Transgenes or constructs were crossed or injected into *psr-1(tm469)* animals, as indicated (*13*). Transgenic embryos were subjected to heat shock (+) at 33°C for 1.5 hours or left at 20°C without heat-shock treatment (−) and scored for the number of cell corpses (mean ± SD) 4 hours after treatment. Average numbers of cell corpses in 15 2-fold stage embryos were determined by Nomarski microscopy. For the P_{hsp}hPSR or P_{hsp}*psr-1*Δ transgene construct (Δ indicates deletion of amino acids 135 to 257 of PSR-1), at least three independent transgenic lines were scored and found to have similar results. The result from one line is shown. As a reference, 9.5 ± 1.6 cell corpses (range 7 to 13 corpses) were seen in 2-fold stage wild-type embryos.

Transgene	Heat shock	No. of corpses	Range of cell corpses
None	−	16.1 ± 4.0	9–23
None	+	16.8 ± 3.8	10–21
$P_{ced\text{-}1}$*psr-1*	−	8.6 ± 1.2	7–11
P_{hsp}*psr-1*	−	16.7 ± 1.7	15–19
	+	8.9 ± 1.6	7–11
P_{hsp}*hPSR*	−	15.5 ± 1.2	14–19
	+	11.5 ± 1.5	9–15
P_{hsp}*psr-1*Δ	−	15.7 ± 0.9	14–18
	+	15.2 ± 1.1	13–18
P_{hsp}*ced-2*	−	15.1 ± 2.2	11–20
	+	9.3 ± 1.7	6–14
P_{hsp}*ced-5*	−	16.1 ± 2.4	12–20
	+	9.2 ± 1.1	8–11
P_{hsp}*ced-10*	−	14.3 ± 1.8	12–19
	+	8.6 ± 1.2	6–10
P_{hsp}*ced-12*	−	16.2 ± 2.8	14–21
	+	8.6 ± 1.2	6–10
P_{hsp}*ced-1*	−	16.2 ± 1.9	13–18
	+	15.9 ± 1.6	14–19
P_{hsp}*ced-6*	−	16.2 ± 2.5	15–21
	+	16.6 ± 2.1	13–19
P_{hsp}*ced-7*	−	16.7 ± 1.7	13–20
	+	16.7 ± 1.4	14−19

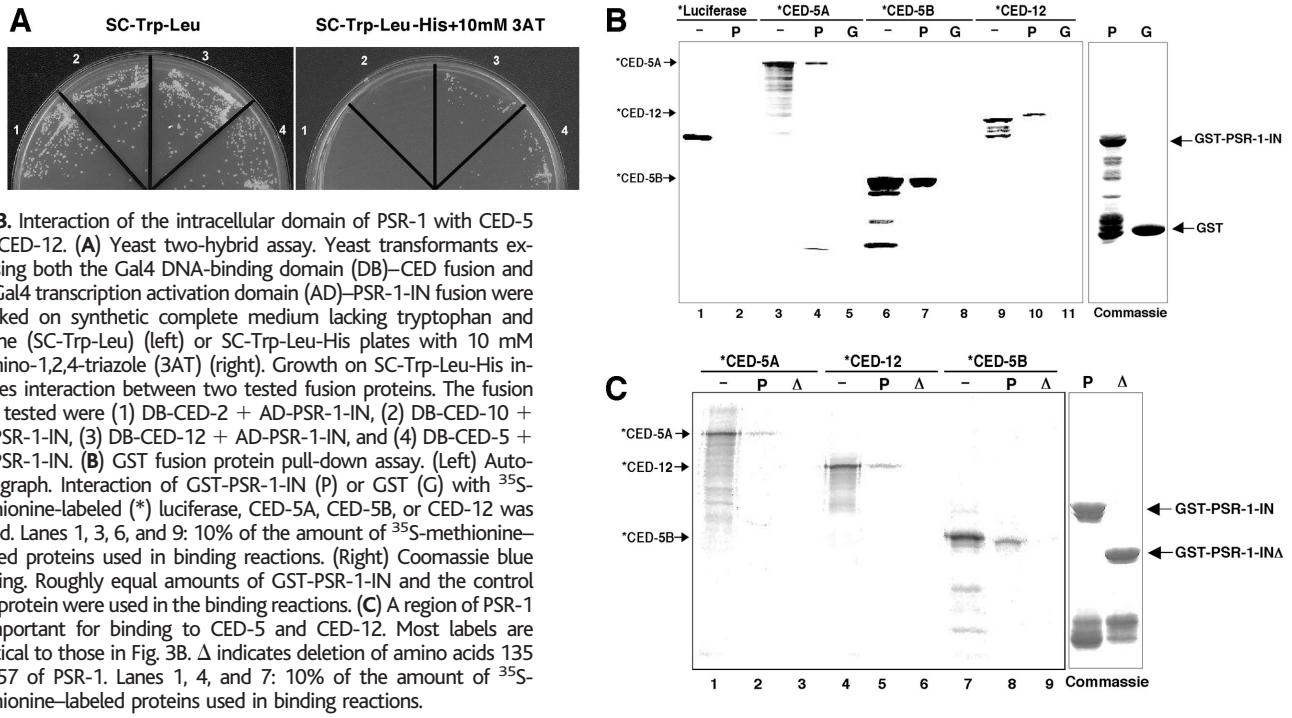

Fig. 3. Interaction of the intracellular domain of PSR-1 with CED-5 and CED-12. (**A**) Yeast two-hybrid assay. Yeast transformants expressing both the Gal4 DNA-binding domain (DB)–CED fusion and the Gal4 transcription activation domain (AD)–PSR-1-IN fusion were streaked on synthetic complete medium lacking tryptophan and leucine (SC-Trp-Leu) (left) or SC-Trp-Leu-His plates with 10 mM 3-amino-1,2,4-triazole (3AT) (right). Growth on SC-Trp-Leu-His indicates interaction between two tested fusion proteins. The fusion pairs tested were (1) DB-CED-2 + AD-PSR-1-IN, (2) DB-CED-10 + AD-PSR-1-IN, (3) DB-CED-12 + AD-PSR-1-IN, and (4) DB-CED-5 + AD-PSR-1-IN. (**B**) GST fusion protein pull-down assay. (Left) Autoradiograph. Interaction of GST-PSR-1-IN (P) or GST (G) with ^{35}S-methionine-labeled (*) luciferase, CED-5A, CED-5B, or CED-12 was tested. Lanes 1, 3, 6, and 9: 10% of the amount of ^{35}S-methionine–labeled proteins used in binding reactions. (Right) Coomassie blue staining. Roughly equal amounts of GST-PSR-1-IN and the control GST protein were used in the binding reactions. (**C**) A region of PSR-1 is important for binding to CED-5 and CED-12. Most labels are identical to those in Fig. 3B. Δ indicates deletion of amino acids 135 to 257 of PSR-1. Lanes 1, 4, and 7: 10% of the amount of ^{35}S-methionine–labeled proteins used in binding reactions.

input), or CED-12 (~2% of input), bound to GST-PSR-1-IN but not to the GST protein alone (Fig. 3B). Thus, PSR-1 appears to interact specifically with CED-5 and CED-12. The intracellular domain of human PSR also bound CED-5 and CED-12, albeit its binding to CED-5A was weaker (fig. S2). These results are consistent with the observation that human PSR can partially rescue the engulfment defect of the *psr-1* mutant. We investigated which region of PSR-1-IN bound CED-5 and CED-12 and found that a C-terminal deletion (amino acids 135 to 257) in PSR-1-IN greatly reduced the binding of PSR-1-IN to both CED-5 and CED-12 (Fig. 3C). Expression of a PSR-1 protein containing this deletion in the *psr-1(tm469)* mutant did not rescue the engulfment defect (Table 1), suggesting that the binding of PSR-1 to CED-5 and CED-12 may be important for the activity of *psr-1* and that PSR-1 may act through CED-5 and CED-12 to promote cell corpse engulfment.

Phagocytosis of apoptotic cells is an integral part of cell death execution and an important event in tissue remodeling, suppression of inflammation, and regulation of immune responses (*25*, *26*). Our observations indicate that *C. elegans* PSR-1, a PS-binding receptor, is important for cell corpse engulfment in vivo and likely transduces the engulfment signal through the CED-5 and CED-12 signaling pathway to promote cell corpse engulfment. However, PSR-1 appears unlikely to be the only engulfment receptor in the *ced-5* and *ced-12* signaling pathway, because the *psr-1* mutant has a weaker engulfment defect than do any of the *ced-2*, *ced-5*, *ced-10*, or *ced-12* mutants. Identification of other engulfment receptors that also act through the *ced-5* and *ced-12* signaling pathway will help to address the fundamental question of how apoptotic cells are recognized and phagocytozed during apoptosis.

References and Notes

1. V. A. Fadok *et al.*, *J. Immunol.* **149**, 4029 (1992).
2. R. F. Ashman, D. Peckham, S. Alhasan, L. L. Stunz, *Immunol. Lett.* **48**, 159 (1995).
3. S. J. Martin *et al.*, *J. Exp. Med.* **182**, 1545 (1995).
4. B. Verhoven, R. A. Schlegel, P. Williamson, *J. Exp. Med.* **182**, 1597 (1995).
5. I. Vermes, C. Haanen, H. Steffens-Nakken, C. Reutelingsperger, *J. Immunol. Methods* **184**, 39 (1995).
6. S. M. van den Eijnde *et al.*, *Cytometry* **29**, 313 (1997).
7. S. M. van den Eijnde, L. Boshart, C. P. M. Reutelingsperger, C. I. De Zeeuw, C. Vermeij-Keers, *Cell Death Differ.* **4**, 311 (1997).
8. S. Krahling, M. K. Callahan, P. Williamson, R. A. Schlegel, *Cell Death Differ.* **6**, 183 (1999).
9. A. Shiratsuchi, S. Osada, S. Kanazawa, Y. Nakanishi, *Biochem. Biophys. Res. Commun.* **246**, 549 (1998).
10. P. R. Hoffmann *et al.*, *J. Cell Biol.* **155**, 649 (2001).
11. V. A. Fadok *et al.*, *Nature* **405**, 85 (2000).
12. V. A. Fadok, A. de Cathelineau, D. L. Daleke, P. M. Henson, D. L. Bratton, *J. Biol. Chem.* **276**, 1071 (2001).
13. Materials and methods are available as supporting material on *Science* Online.
14. J. Parrish *et al.*, *Nature* **412**, 90 (2001).
15. X. C. Wang, D. Xue, unpublished results.
16. L. C. Cheng, Y. C. Wu, unpublished results.
17. Z. Zhou, E. Hartwieg, H. R. Horvitz, *Cell* **104**, 43 (2001).
18. R. E. Ellis, D. M. Jacobson, H. R. Horvitz, *Genetics* **129**, 79 (1991).
19. Y. C. Wu, M. C. Tsai, L. C. Cheng, C. J. Chou, N. Y. Weng, *Dev. Cell* **1**, 491 (2001).
20. Z. Zhou, E. Caron, E. Hartwieg, A. Hall, H. R. Horvitz, *Dev. Cell* **1**, 477 (2001).
21. T. L. Gumienny *et al.*, *Cell* **107**, 27 (2001).
22. Y. C. Wu, H. R. Horvitz, *Nature* **392**, 501 (1998).
23. P. W. Reddien, H. R. Horvitz, *Nature Cell Biol.* **2**, 131 (2000).
24. E. Brugnera *et al.*, *Nature Cell Biol.* **4**, 574 (2002).
25. J. Savill, V. Fadok, *Nature* **407**, 784 (2000).
26. P. M. Henson, D. L. Bratton, V. A. Fadok, *Curr. Biol.* **11**, R795 (2001).
27. T. Nakano *et al.*, *J. Biol. Chem.* **272**, 29411 (1997).
28. V. Fadok, unpublished results.
29. J. E. Sulston, E. Schierenberg, J. G. White, J. N. Thomson, *Dev. Biol.* **100**, 64 (1983).

30. We thank M. Han, Y. Kohara, and Z. Zhou for reagents and strains; M. Valencia and V. Zapata for help with statistical analysis; and B. Wood and L. Edgar for help with four-dimensional microscopy analysis. This research was supported in part by the Searle Scholar Award and the Burroughs Wellcome Fund Career Award (D.X.), and grants from the Ministry of Education (89-B-FA01-1-4) and National Science Council of Taiwan (Y.-C.W.); the Ministry of Education, Culture, Sports, Science and Technology of Japan (S.M.); and NIH (D.X. and V.A.F.).

Supporting Online Material

www.sciencemag.org/cgi/content/full/302/5650/1563/DC1
Materials and Methods
Figs. S1 and S2
References

5 June 2003; accepted 8 October 2003

Fish Exploiting Vortices Decrease Muscle Activity

James C. Liao,[1]* David N. Beal,[2] George V. Lauder,[1] Michael S. Triantafyllou[2]

Fishes moving through turbulent flows or in formation are regularly exposed to vortices. Although animals living in fluid environments commonly capture energy from vortices, experimental data on the hydrodynamics and neural control of interactions between fish and vortices are lacking. We used quantitative flow visualization and electromyography to show that trout will adopt a novel mode of locomotion to slalom in between experimentally generated vortices by activating only their anterior axial muscles. Reduced muscle activity during vortex exploitation compared with the activity of fishes engaged in undulatory swimming suggests a decrease in the cost of locomotion and provides a mechanism to understand the patterns of fish distributions in schools and riverine environments.

Many fishes live in habitats in which they commonly encounter vortices that arise from fluid flow past stationary objects or from the propulsive movements of other animals. Energy extraction from environmental vortices has been consistently implicated as a hydrodynamic mechanism to increase the performance of swimming fishes (*1*–*8*). The preference of fishes to use these unsteady flows has been documented in the field (*4*, *9*, *10*) and laboratory (*11*–*13*). However, the dynamic and transparent nature of flowing water has precluded quantitative visualization of interactions between fishes and vortices and, thus, an understanding of the underlying physical mechanisms involved. Furthermore, the effect of vortical flows on the degree and pattern of axial muscle activity in fishes remains entirely unknown.

We generated periodic vortices of similar strength and size to each other by using a vertically mounted D-section cylinder (i.e., a cylinder bisected along its long axis) placed in water flowing at a known velocity (*14*) (Fig. 1). These vortices were shed from the D-section cylinder in a staggered array collectively known as a Kármán street (*15*). A Kármán street is an example of a drag wake (rotation of alternately shed vortices is toward each other upstream), which can form between the thrust wakes (rotation of alternately shed vortices is toward each other downstream) of two fish swimming side by side (*5*). Vortices generated by the D-section cylinder were similar in strength to those produced by other freely swimming fish (*16*, *17*).

Compared with swimming in free stream (uniform) flow, there are two hydrodynamic benefits of station holding behind a cylinder. Fish can simply swim against the current in the region of reduced flow, drafting, for example, as a bicyclist would behind another bicyclist, or they can generate lift to move against the flow by altering their body kinematics to synchronize with the shed vortices. Because energy can be captured from cylinder vortices (*18*), trout that synchronize their body kinematics to vortices appropriately may need to use very little energy and, thus, gain a hydrodynamic advantage beyond that of drafting in the reduced velocity alone.

[1]Department of Organismic and Evolutionary Biology, Harvard University, Cambridge, MA 02138, USA. [2]Department of Ocean Engineering, Massachusetts Institute of Technology, Cambridge, MA 02139, USA.

*To whom correspondence should be addressed: E-mail: jliao@oeb.harvard.edu